Electronic Supplementary Material (ESI) for Lab on a Chip.

SUPPLEMENTARY

Optomicrofluidic detection of cancer cells in peripheral blood via metabolic glycoengineering

K. Mirkale[1,*], S. K. Jain[1], T. S. Oviya[1], S. Mahalingam[2]

[1]Micro Nano Bio Fluidics Unit, Department of Mechanical Engineering, Indian Institute of Technology Madras, Chennai-600036, Tamilnadu, India.

[2] Laboratory of Molecular Cell Biology, National Cancer Tissue Biobank, Department of Biotechnology, Bhupat and Jyoti Mehta School of Biosciences, Indian Institute of Technology Madras, Chennai-600036, India

[*]Author to whom correspondence should be addressed. Email: kshitija.mirkale@gmail.com

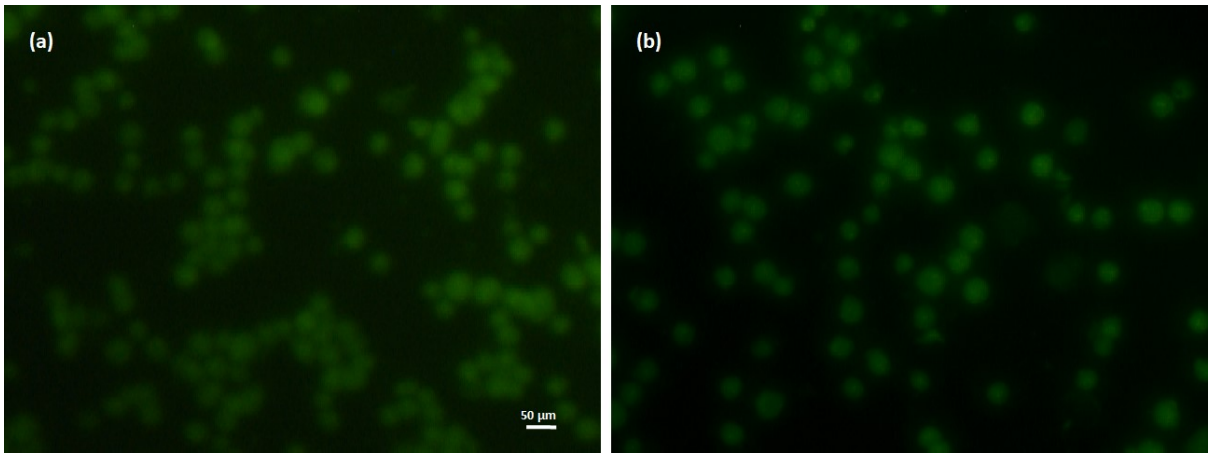

Fig. S1. Fluorescence signal obtained when cells incubated with (a) 50µM sodium azide (b) 50µM Ac_4ManNAz, overnight and later treated with 50 µM AZDye 488 DBCO for 1hour

S1. Optomicrofluidic detection of metabolically tagged CTCs – 1D cell focusing

In the initial stage of study, cells were focused in a single dimensional plane by simple hydrodynamic focusing, as shown in Figure S2. The width of the focused stream (w_s) depended on the ratio (r) of sheath flow rate (Q_{sh}) and sample flow rate (Q_s). It was observed that w_s decreased with an increase in r and is correlated as $w_s = r^{-0.976}\mu m$ ($R^2 = 0.976$). To completely focus cells in a single file, w_s should be close to the smallest cell size. At the same time, cell concentration and flow rates should be chosen such that no two cells should pass through the optical detection region simultaneously. Hence, we chose a lower throughput condition (100 cells/min) to demonstrate detection.

When the cell passes through the optical detection region, it is excited by the source fibre, causing the generation of different signals like fluorescence (FL) and scatter signals. In a flow cytometer, there are two types of scattered signals forward scatter signal (FSC) and side scatter signal (SSC). Height or area of the FSC signal depends on the size of the object, bigger is the object more it can obstruct the laser beam. While side scattered light depends on the internal complexity and granularity of the object. When cancer cell passes through the optical detection region, it generates an FSC signal greater than the FSC signal generated by PBMC. This is because of the difference in size ranges observed in different cell lines (Table 1). The performance of the 1-D focused micro-flow cytometer in terms of scattered signals (Fig. S4) is satisfactory and comparable to literature[1]. Each signal (FL, FSC, SSC) is normalized by the background noise signal (Fig. S3, S4). Few fluorescent molecules in cell

suspension media were observed even after performing two PBS washes after tagging. This is because of hydrolyzation of glycans by neuraminidase resulting in disappearing azide groups from the cell surface as observed in other studies[2]. Hence, focusing cells along with fluorescent suspension media by sheath fluid into a narrower stream helped to reduce background noise.

However, we cannot rule out the possibility of cells flowing through different heights of the channel. This results in non-uniform velocity distribution of cells and hence non-uniform residence time, causing variation in optical signals[3]. Also, cells at different heights can experience a different amount of excitation and emission. Due to these reasons, we observed that some of the cancer cells could not produce a significant amount of fluorescence even after being tagged well (Fig. S4). Two or more cells passing through different heights simultaneously disturb the objective of single-cell detection. Hence, we proceeded to first improve the cell focusing method.

The performances of the 2D hydrodynamic focusing and droplet encapsulation schemes are compared in terms of the coefficient of variation (CV) of optical signals obtained from the cells. As droplets containing PBMCs were not easily differentiable from empty droplets, these droplets are not considered for analysis for CV. As the droplet encapsulation scheme offers 2D focusing of cells ensuring single-file movement of cells through the detection region, the the FL signals obtained in this case is smaller than the hydrodynamic focusing case. The CV of FL signals obtained in droplet focusing scheme is found to be about half as compared to the 2D hydrodynamic focusing case (see table S1). The CV of the FL signals for the droplet encapsulated cells is attributed to the heterogeneous nature of the CTCs[4]. For the droplet encapsulation case, the CV of FSC signals is found to be very small as the FSC signal largely depends on the droplet size which has a uniform distribution. While the background noise is found to be lower for MCF7 and MDA-MB-231 compared to HeLa, scatter plots for all CTCs were observed to be similar as the FL intensity normalization against the background signals.

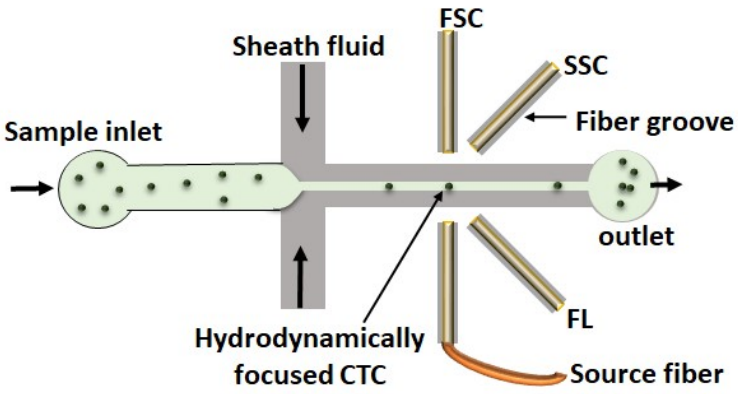

Fig. S2 Schematic diagram showing optomicrofluidic detection of CTCs – cells are focused hydrodynamically by sheath fluid (© 2023 IEEE. Adapted, with permission, from [Mirkale K. et. al.[6]]).

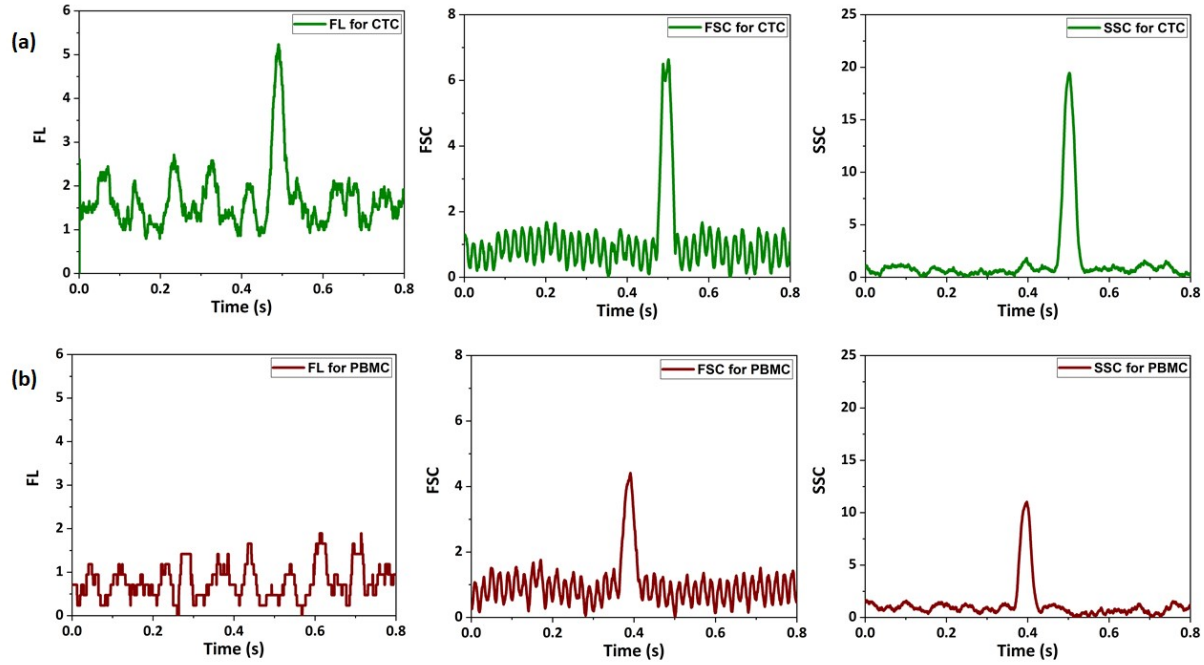

Fig. S3 The time-variations of fluorescence (FL), forward scatter (FSC), and side scatter (SSC) signals for (a) HeLa cells and (b) PBMCs. In each case, the signal intensity is normalized with the corresponding background signal intensity.

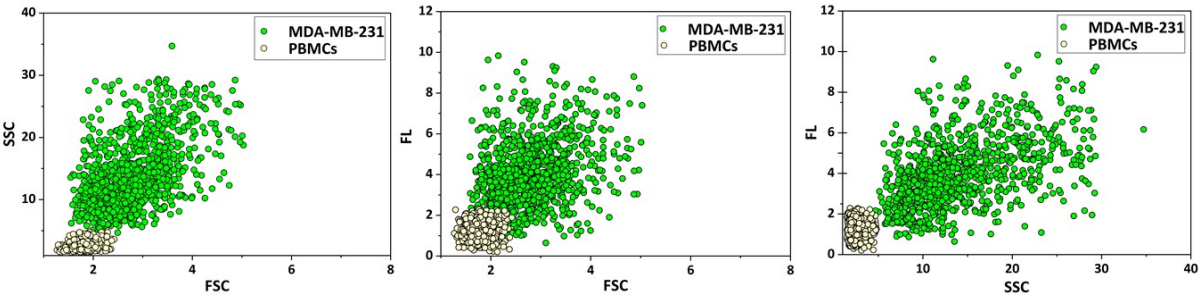

Fig. S4 Scatter plots for PBMCs and MDA-MB-231. Optical signal intensity is normalized with the background noise

Table S1: Coefficient of variation (CV) of FL signal in case of droplet encapsulated (2D focused) and hydrodynamically focused (1D focused) cells

Cell type	CV of FL signal	
	2D focused	1D focused
HeLa	15.70	29.86
MCF7	17.59	35
MDA-MB-231	19.05	40.78

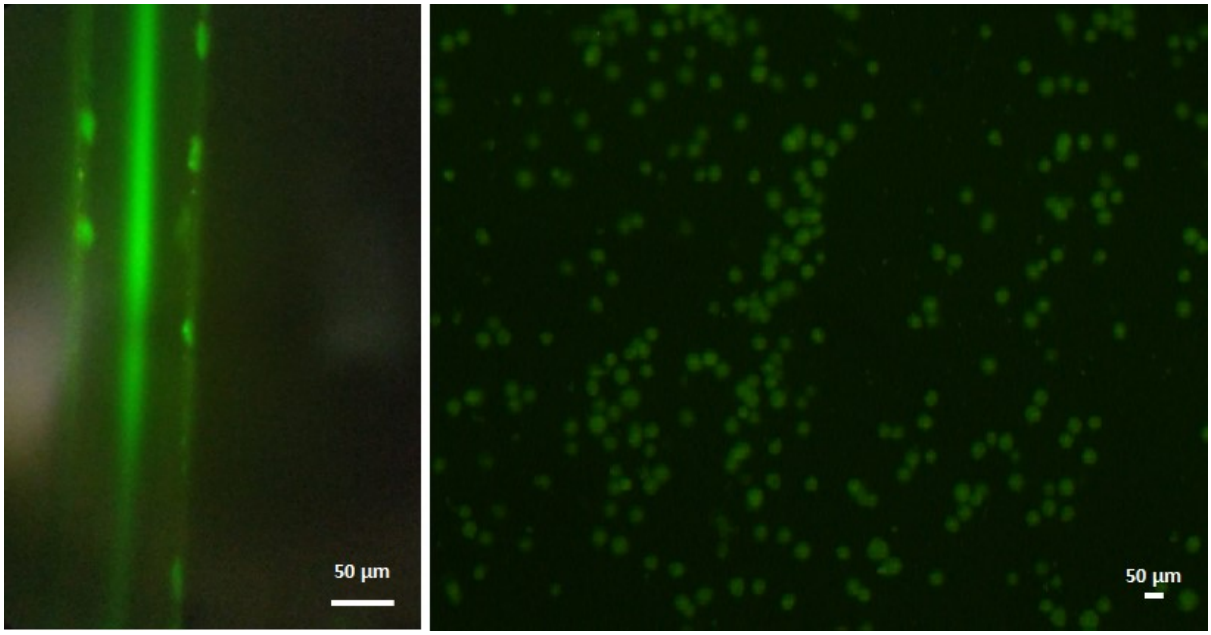

Fig. S5 FL images showing traces of fluorescent molecules in (a) 1D focused stream of the fluorescent cell suspension media inside channel observed under fluorescence lamp even after performing two PBS washes following tagging. (b) cell image with background fluorescence

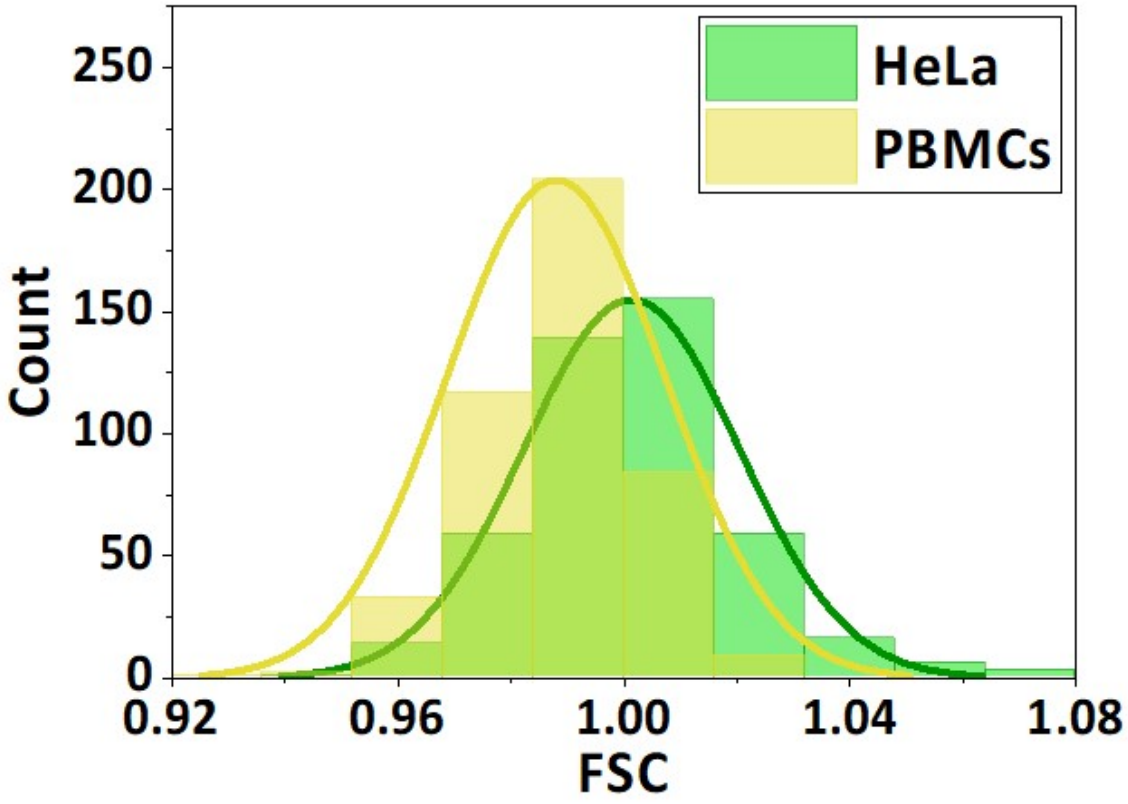

Fig. S6 A comparison of the heights of the FSC signal peaks for the cancer cells and PBMCs indroplet encapsulation scheme.

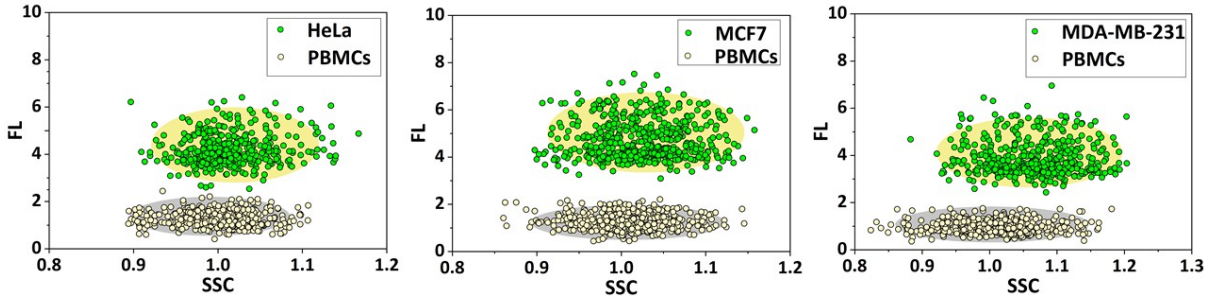

Fig. S7 The FL-SSC scatter plots for the different types of CTCs and PBMCs encapsulated in droplets.

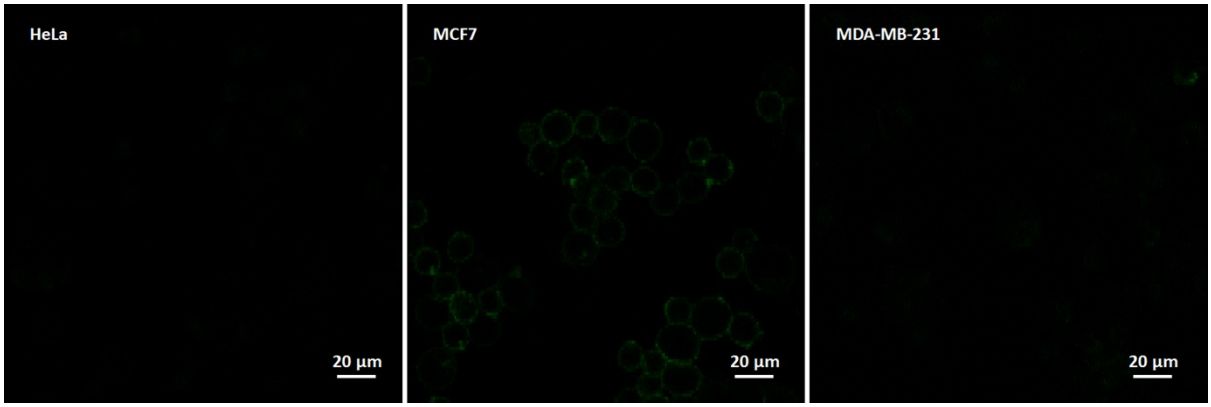

Fig. S8 Fluorescence images of cells tagged with Anti-EpCAM-FITC

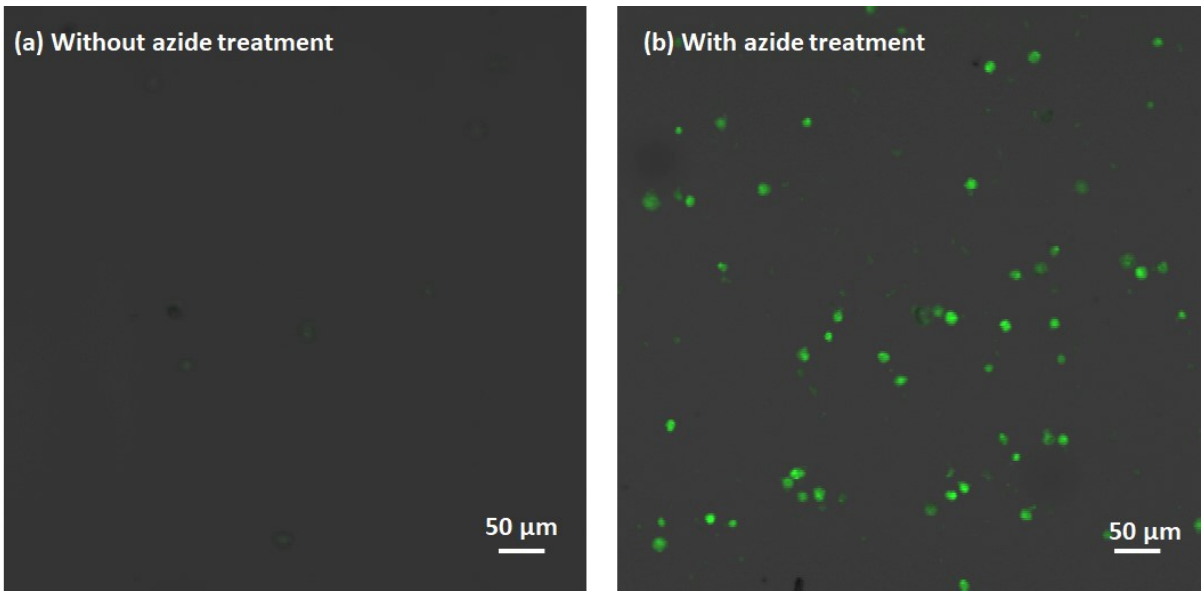

Fig. S9 Merged confocal images of cells tagged with AZDye 488 DBCO (a) without azide treatment (b) with azide treatment

S2. Optical simulation

As fluorescence signal is weakest, it is necessary to ensure optical loss of FL signal is not significant when cell is encapsulated inside droplet. To estimate average power loss from source to detector we performed optical wave propagation simulation using 'Electromagnetic Waves, Beam Envelopes' physics interface. The optimized mesh for our study was of the type unstructured triangular mesh with maximum element size used 4 µm. Wave equation for electric field envelope is given by

$$(\nabla - ik_1) \times ((\nabla - ik_1) \times E) - k_0^2\left(\varepsilon_r - \frac{i\sigma}{\omega\varepsilon_0}\right)E = 0$$

Where k_1 is wave vector, E is electric field envelope function, k_0 is wave number of signal in vacuum, ε_r is relative permittivity of fluid, ε_0 is permittivity of free space, σ is electrical conductivity of fluid, ω is frequency of wave. The optimized mesh for our study was of the type triangular with maximum element size used was 1 µm. To define boundary condition in between two different domains of fluid, Electric displacement field model of refractive index was used. Where refractive index is complex entity given by

$$\bar{n} = n - jk$$

Where n is real part of refractive index which was estimated by refractometer (Rudolph Research Analytical, USA) k is imaginary part of refractive index estimated by knowing the values of electrical conductivity (σ) and electrical permittivity ($\varepsilon = \varepsilon_0\varepsilon_r$) of material.

$$\sqrt{\bar{\varepsilon}_r} = n - jk$$

$$\bar{\varepsilon}_r = (n - jk)^2$$

$$\varepsilon_r - j\frac{\sigma}{\omega\varepsilon} = n^2 - k^2 + 2jnk$$

$$\varepsilon_r - j\frac{\sigma}{\omega\varepsilon} = n^2 - k^2 + 2jnk$$

$$\frac{\sigma}{\omega\varepsilon} = 2nk$$

A gaussian beam with peak electric field 1V/ m is given as input source. Input source is place at Center of the width of the channel assuming cell is focused at center. 2D model has been developed representing central plane of the channel (height wise) assuming cell is focused there. But this is not always the case in hydrodynamic cell focusing scheme and power loss can be more depending on position of cells. Power loss is expected to be maximum when cell is near top wall or bottom wall of channel. But these effects are not incorporated in this simulation, a complete 3-dimensional modelling is required which can incorporate such multiple parameters which is beyond scope of this work.

We observed scattering of light as it enters another domain due to sudden change in refractive index, also we observed some fringe like patterns at the interfaces as mentioned in literature[5].

Material	σ (S/m)	ε_r	n
PBS1 (PBS +5 % PEG)	2	79	1.388
PBS1 (PBS +18% Optiprep)	2	79	1.3443
Mineral oil	10^{-12}	2.1	1.48
PDMS	$1.71X10^{-12}$	2.69	1.43

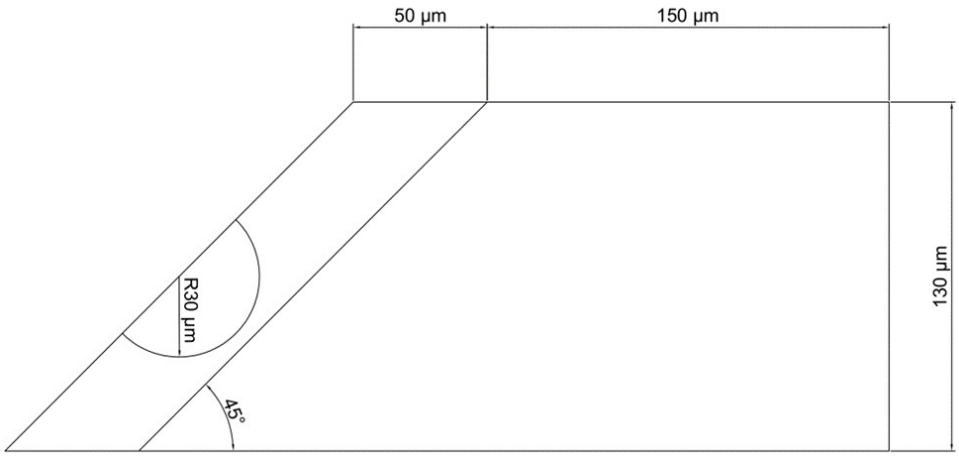

Fig. S10: Numerical simulation domains with dimensions

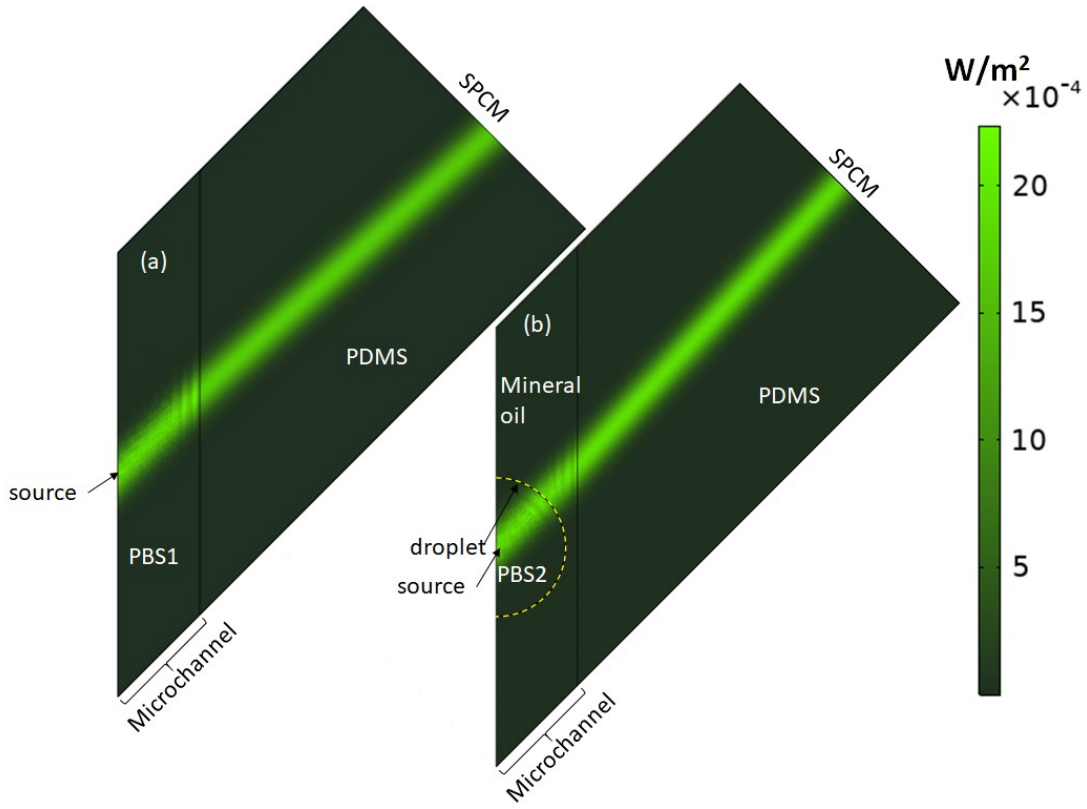

Fig. S11: Optical power propagation profile from cell to SPCM detector in (a) hydrodynamic 1D focusing scheme (b) droplet encapsulation 2D focusing scheme (© 2023 IEEE. Adapted, with permission, from [Mirkale K. et. al.[6]].

References:

1. Spencer, D., Hollis, V. & Morgan, H. Microfluidic impedance cytometry of tumour cells in blood. *Biomicrofluidics* **8**, (2014).

2. Layek, B., Sadhukha, T. & Prabha, S. Glycoengineered mesenchymal stem cells as an enabling platform for two-step targeting of solid tumors. *Biomaterials* **88**, 97–109 (2016).

3. Gaikwad, R. & Sen, A. K. An optomicrofluidic device for the detection and isolation of drop-encapsulated target cells in single-cell format. *Analyst* **146**, 95–108 (2021).

4. Denison, T. A. & Bae, Y. H. Tumor heterogeneity and its implication for drug delivery. *J. Control. Release* **164**, 187–191 (2012).

5. Yu, J. Q. *et al.* Droplet optofluidic imaging for λ-bacteriophage detection via co-culture with host cell Escherichia coli. *Lab Chip* **14**, 3519–3524 (2014).

6. Mirkale, K. & Sen, A. K. Advantage of droplet encapsulation scheme in microflow cytometer based detection. *APSCON 2023 - IEEE Appl. Sens. Conf. Symp. Proc.* 1–3 (2023) doi:10.1109/APSCON56343.2023.10100972.